Impact of Reconfiguration and Network Topology on Voltage Stability Margin

V. V. S. N. Murty Vallem and Ashwani Kumar

Abstract This paper presents the impact of feeder reconfiguration and network topology on voltage stability margin in distribution sytems. This work includes: (i) voltage stability margin analysis in mesh network and reconfigured distribution system, (ii) a new stability index is established for mesh networks, (iii) voltage stability margin is determined for various voltage-dependent load models, (iv) voltage stability margin enhancement is studied with PV penetration and OLTC, (v) probabilistic load model and uncertainty of PV power output are also taken care in the evaluation of voltage stability margin. The analysis has been conducted on IEEE 33-bus distribution network.

Keywords Distribution system · Reconfiguration · Mesh distribution system · Load models · Voltage stability margin · OLTC · Distribution generation

1 Introduction

Power system operating point should be stable, secure and meeting various operational constraints under normal and contingency scenarios. However, due to economical and environmental constraints, the present power system networks are highly stressed and weak and are being operated at the verge of stability limits. İn this scenario, maintaining the voltage stability is a challenging task for the system operator which is essential for power system planning and operational aspect. The popular topology of distribution system is radial structure. However, meshed topology is also used to provide reliable system for areas with heavy load density. Many authors have focussed reconfiguration problem and mesh topolgy for reduction in energy loss and voltage drop. In addition to this, voltage stability margin investigation is another essential aspect must be analysed. Voltage instability means fall in bus voltage below

---

V. V. S. N. Murty Vallem (✉) · A. Kumar
Department of Electrical Engineering, NIT Kurukshetra, Kurukshetra, Haryana, India
e-mail: murty209@gmail.com

A. Kumar
e-mail: ashwani.k.sharma@nitkkr.ac.in

M. J. B. Reddy et al. (eds.), *Advances in Smart Grid Automation and Industry 4.0*, Lecture Notes in Electrical Engineering 693, https://doi.org/10.1007/978-981-15-7675-1_45

its rated value due to outage of generator, transformer, line, overloading and reactive power deficiency [1, 2]. Driving factors for voltage instability are outage of lines, generators and transformers. In addition to this, inadequate reactive power support, radial configuration of the system, affects voltage stability. Sudden disturbances of reactive power demand drive the system into instability region. Voltage stability of the system can be enhanced with adequate reactive power compensation, load shedding during contingencies, parallel lines. Distribution network operator at control centre needs to monitor change in load demand, bus voltage and reactive power reserve closely. Various conventional approaches such as PV curve, QV curve, continuous power flow [3, 4] and singularity of jacobian matrix [5–7] exist to analyse voltage stability phenomenon. Branch equivalent was adopted for network reduction [8]. Static stability index was formulated for radial system based on network load admittance ratio [9] and loop system [10]. The effect of network topology and reconfiguration in standalone microgrids has been studied for small signal stability [11]. In reconfiguration, network topology is modified by opening/closing tie lines to minimise power loss, improve voltage profile [12, 13], maximisation of loadability [14]. Reconfiguration of islanded microgrids presented in [15, 16] for loss minimisation and loadability maximisation. Maximum allowable loading values were determined in radial distribution system subject to voltage stability [17]. Various static voltage stability indices were presented in [18, 19]. Voltage stability margin improvement was addressed with distribution generation [20].

The rest of this paper is organised as follows. The proposed stability index is presented in Sect. 2. In Sect. 3, simulation results are provided. Finally, conclusions of this work are given in Sect. 4.

2 Proposed Voltage Stability Index

A simple mesh distribution system with three loops is shown in Fig. 1. Load flow equations for mesh distribution system are described below and new voltage stability index is established for mesh system using power flow equations (Fig. 2).

The effective power at each node is calculated as follow:

Apply Kirchhoff's voltage law in each loop:

For loop1:

$$\begin{aligned} &ZL_{34} * \left\{\left[Pe(4)' + jQe(4)'\right]/V(4)\right\}5^{*} + ZL_{45} * \left\{\left[Pe(5)' + jQe(5)\right]/V(5)\right\}^{*} \\ &\quad - ZL_{36} * \left\{\left[Pe(6)' + jQe(6)'\right]/V(6)\right\}^{*} + ZL_{56} * I_{\text{loop}}(1) = 0 \end{aligned} \tag{1}$$

$$\begin{aligned} &ZL_{34} * \left(\{[Pe(4) + jQe(4)]/V(4)\}^{*} + I_{\text{loop}}(1) - I_{\text{loop}}(2)\right) \\ &\quad + ZL_{45} * \left(\{[Pe(5) + jQe(5)]/V(5)\}^{*} + I_{\text{loop}}(1) - I_{\text{loop}}(2)\right) \end{aligned}$$

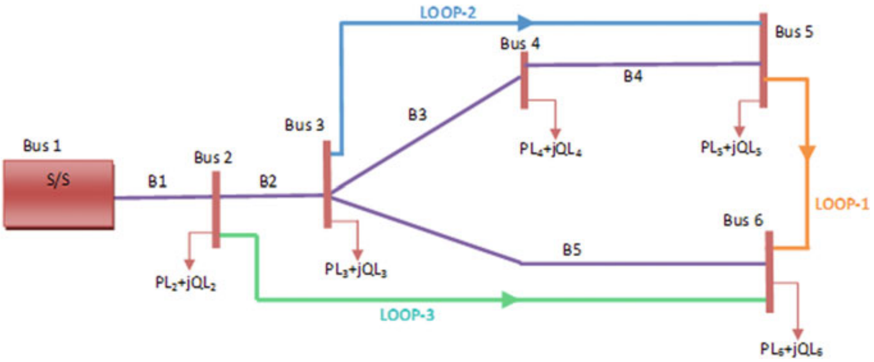

Fig. 1 Typical loop distribution system

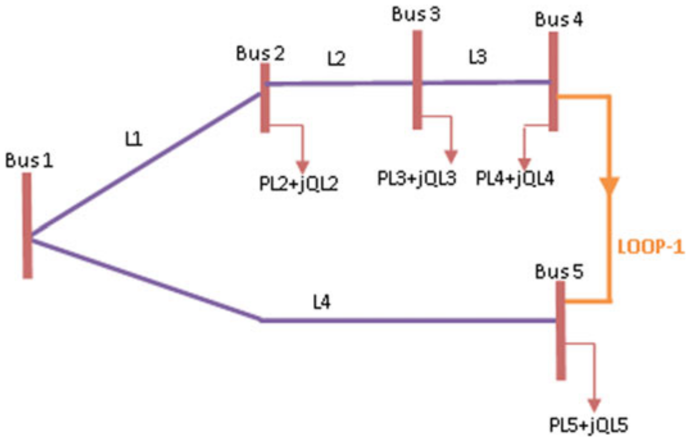

Fig. 2 Single mesh distribution system

$$- ZL_{36} * \left(\{[Pe(6) + jQe(6)]/V(6)\}^{*} - I_{\text{loop}}(1) - I_{\text{loop}}(3)\right) + ZL_{56} * I_{\text{loop}}(1) = 0 \tag{2}$$

$$\begin{aligned}&\left((ZL_{34} + ZL_{45} + ZL_{36} + ZL_{56}) * I_{\text{loop}}(1)\right) - \left((ZL_{34} + ZL_{45}) * I_{\text{loop}}(2)\right) + ZL_{36} * I_{\text{loop}}(3)\\&\quad = -\left(ZL_{34} * \{[Pe(4) + jQe(4)]/V(4)\}^{*} + ZL_{45} * \{[Pe(5) + jQe(5)]/V(5)\}^{*}\right.\\&\qquad \left.-ZL_{36} * \{[Pe(6) + jQe(6)]/V(6)\}^{*}\right)\end{aligned} \tag{3}$$

For loop 2:

$$\begin{aligned}&- \left((ZL_{34} + ZL_{45})*I_{\text{loop}}(1)\right) - \left((ZL_{34} + ZL_{45} + ZL_{35})*I_{\text{loop}}(2)\right)\\&\quad = -\left(-ZL_{34}*\{[Pe(4) + jQe(4)]/V(4)\}^{*}\right.\\&\qquad \left.-ZL_{45}*\{[Pe(5) + jQe(5)]/V(5)\}^{*}\right)\end{aligned} \tag{4}$$

For loop 3:

$$\begin{aligned}&\big(ZL_{36}{*}I_{\text{loop}}(1)\big) + \big((ZL_{23} + ZL_{36} + ZL_{26}){*}I_{\text{loop}}(3)\big)\\&\quad = -\big(-ZL_{23}{*}\{[Pe(3) + jQe(3)]/V(3)\}^{*}\\&\qquad -ZL_{36}{*}\{[Pe(6) + jQe(6)]/V(6)\}^{*}\big)\end{aligned} \tag{5}$$

$$[Zloop]{*}I_{\text{loop}} = -[VDloop] \tag{6}$$

$$I_{\text{loop}} = [Zloop]^{-1}{*}[-VDloop] \tag{7}$$

$$P(5) - j * Q(5) = I_{\text{loop}} * V_5^{*} \tag{8}$$

$$\begin{aligned}(ZL_{12} + ZL_{23} + ZL_{15} + ZL_{34} + ZL_{45})I_{\text{loop}} = {}&-ZL_{12}\left(\frac{Pe(2) + j * Qe(2)}{V(2)}\right)^{*}\\&- ZL_{23}\left(\frac{Pe(3) + j * Qe(3)}{V(3)}\right)^{*}\\&- ZL_{34}\left(\frac{Pe(4) + j * Qe(4)}{V(4)}\right)^{*}\\&- ZL_{15}\left(\frac{Pe(5) + j * Qe(5)}{V(5)}\right)^{*}\end{aligned} \tag{9}$$

$$(ZL_{12} + ZL_{23} + ZL_{15} + ZL_{34} + ZL_{45})I_{\text{loop}} = -(V(1) - V(5)) \tag{10}$$

$$P(5) - j * Q(5) = -\frac{(V(1) - V(5))}{(Z_{12} + Z_{23} + Z_{14} + Z_{34} + Z_{45})} * V_4^{*} \tag{11}$$

$$ZL = (ZL_{12} + ZL_{23} + ZL_{14} + ZL_{34} + ZL_{45}) = R + jX \tag{12}$$

$$(P - jQ)(R + jX) = V_5^2 - V_1V_5\cos\delta - jV_1V_5\sin\delta \tag{13}$$

$$V_5^2 - V_1V_5\cos\delta = PR + QX \tag{14}$$

$$V_1V_5\sin\delta = QR - PX \tag{15}$$

$$P = \frac{QR - V_1V_5\sin\delta}{X} \tag{16}$$

$$V_5^2 - V_1V_5\cos\delta = \frac{QR - V_1V_5\sin\delta}{X}R + QX \tag{17}$$

$$V_5^2 + V_1 V_5\left[-\cos\delta + \frac{R\sin\delta}{X}\right] - Q\left[X + \frac{R}{X}\right] = 0 \tag{18}$$

$$V_1^2(\sin(\delta - \theta))^2 \geq -4Q\sin\theta^2\left[X + \frac{R}{X}\right]^2 \tag{19}$$

$$1 \geq \frac{4Q\sin\theta^2\left[X + \frac{R}{X}\right]^2}{V_1^2(\sin(\delta - \theta))^2} \tag{20}$$

$$\text{new VSI} = \frac{4Q\sin\theta^2\left[X + \frac{R}{X}\right]^2}{V_1^2(\sin(\delta - \theta))^2} \tag{21}$$

Under normal operating condition, value of VSI should be <1. At the point of voltage collapse, VSI value closer to 1. Based on proposed new VSI, weak node is 30th bus for the test system.

3 Simulation Results

Simulation results have been obtained on IEEE 33-bus distribution system having five loops with various voltage-dependent load models. The influence of number of loops in mesh netwrok and feeder reconfiguration has been investigated for voltage stability margin. Based on real-time experience, critical voltage for voltage collapse is considered as 80% of rated voltage. Critical real power loading (m_p), reactive power loading (m_q) and complex power loading are determined for radial distribution system considering reconfiguration and mesh topology. Further, stochastic nature of load demand is modelled using normal distribution function and PV power output is modelled using beta distribution function. Voltage stability margin values are determined for various load models, reconfiguration and number of loops of meshed distribution system. It is observed from the simulation studies that reconfiguration, load model, network structure, DG penetration and OLTC have significant impact on voltage stability margin.

3.1 Reconfigured Distribution System

Shortest optimal path is determined in reconfigured distribution system using genetic algorithm. Open switches are: 7, 9, 14, 32, 37. In reconfigured distribution system, power loss and voltage drop are lower than base case system. Summary of results is given in Table 1 for various load models in terms of critical bus voltage, power loss and maximum allowable loading. It is understood from Table that voltage stability margin is improved with reconfiguration. Maximum permissible loading is higher

Table 1 Voltage stability margin in reconfigured radial distribution system

	CP	CI	CZ	ZIP
Voltage (p.u) at 30th bus	0.93884	0.94218	0.94501	0.94242
TPL (kW)	139.55	127.36	117.28	132.21
m_{p} (kW)	3260	4420	5880	4450
m_{q} (kVAr)	4160	5640	7500	5680
m_{s} (kVA)	2743.5	3747.6	5006.3	3775.9

for CZ load model than other load models as mentioned in Table 1. Also, PV and QV curves in reconfigured distribution system are shown in Figs. 3 and 4.

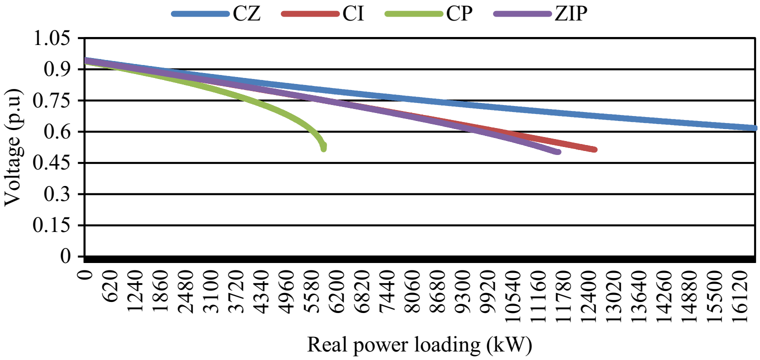

Fig. 3 Voltage profile with real power loading in reconfigured distribution system

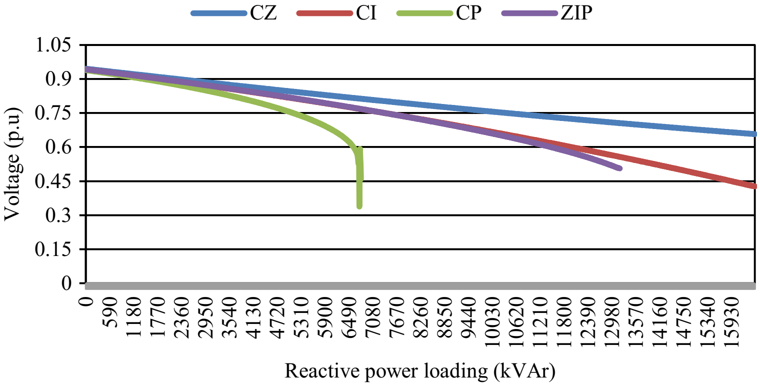

Fig. 4 Voltage profile with reactive power loading in reconfigured distribution system

3.2 *Mesh Distribution System*

Voltage stability margin analysis has been studied for mesh distribution system with five loops and noticed that stability margin is high for five loops case. P–V and Q–V curves for mesh network are shown in Figs. 5 and 6. Comparison of stability margin for radial and mesh topology is given in Table 2 for various voltage-dependent load models. As specifed in Table 2, the least stability margin values are noticed for CP load model and highest stability margin values are observed for CZ load model. Better voltage profile with reduced power losses is seen in mesh network compared to radial structure (RDS). Consequently, mesh topogy has better stability margin compared to radial distribution systems.

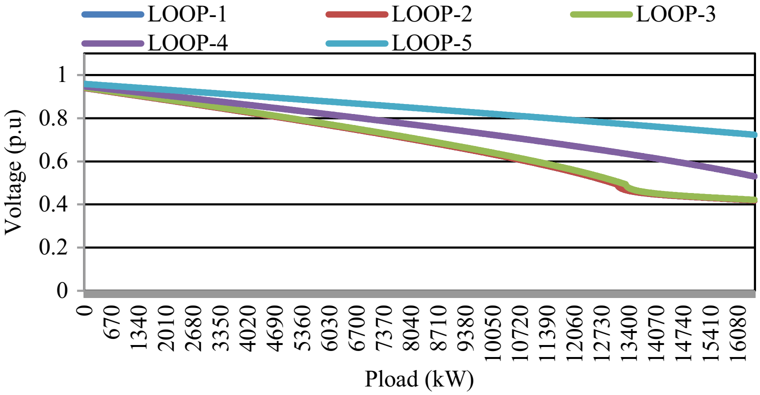

Fig. 5 Voltage profile with real power loading in mesh distribution system

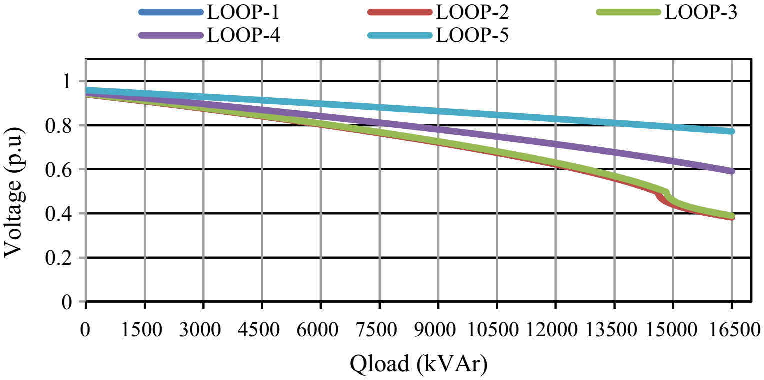

Fig. 6 Voltage profile with reactive power loading in mesh distribution system

Table 2 Voltage stability margin in radial andmesh distribution system

	CP		CI		CZ		ZIP	
	RDS	Mesh	RDS	Mesh	RDS	Mesh	RDS	Mesh
V_{30} (p.u)	0.92195	0.9569	0.9275	0.9585	0.9320	0.9600	0.9278	0.9587
TPL (kW)	202.66	123.28	176.63	114.42	156.87	106.78	174.94	113.71
m_{p} (kW)	2840	8680	3980	11,350	5400	14,710	4010	11,430
m_{q} (kVAr)	3660	10,880	5110	14,220	6930	18,400	5150	14,310
m_{s} (kVA)	2390.0	7339.7	3365.8	9630.7	4596.1	12,487.5	3394.1	9687.3

3.3 DG Penetration

In this case study, maximum loadability enhancement is studied with penetration of PV-based inverter distribution generation having real and reactive power support. Three DGs are strategically installed at 6th bus (945 kVA @0.85 pf), 14th bus (1285 kVA @0.85 pf) and 30th bus (1240 kVA @0.85 pf). The power loss is reduced significantly and voltage regulation is maintained within permisisble range with DG placement. In addition to this, maximum allowable loading is increased to 8820 kVA with DG installation.

3.4 OLTC

In this case study, impact of OLTC tap position is investigated on voltage stability margin enhancement in mesh distribution systems. OLTC with five steps from −5% to +5% variations in steps of 2.5% is considered. Under normal operating scenario, OLTC tap position is set at nominal tap position ‘3’. Voltage variation with real and reactive power loading considering OLTC action is shown in Fig. 7.

4 Conclusion

In this paper, a detailed analysis is presented to assess the impact of feeder reconfiguration, network topology and load models on voltage stability margin in distribution systems considering unceratnty factors. Further, a new static voltage stability index is developed for mesh distribution systems. Impact of number of loops on voltage stability margin is explored in this work. It has been observed that voltage profile is better in mesh networks compared to radial topology. Also, in mesh network, the real power loss is lower compared to radial topology. Numerical results indicate that

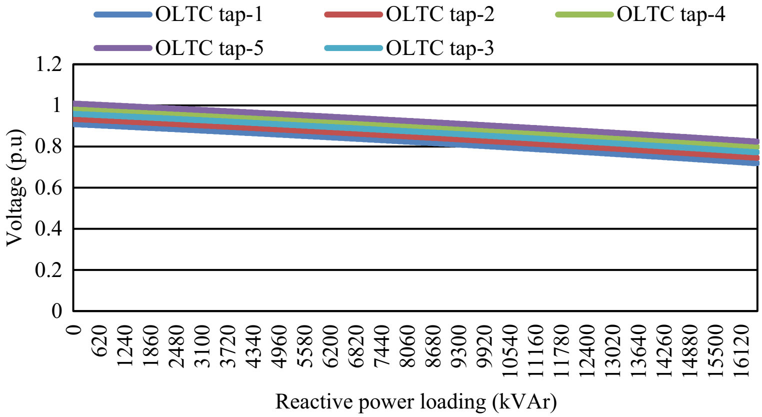

Fig. 7 Variation of bus voltage with reactive power loading against OLTC operation

mesh network has higher voltage stability margin values compared to radial structure. Voltage stability margin is increased with penetration of distribution generation, reconfiguration and OLTC.

This study provides guidelines to distribution network operator for optimal reactive power management and DG integration in reconfigured distribution systems taking into account of voltage stability margin constraint.

References

1. Taylor CW (1994) Power system voltage stability. McGraw-Hill
2. Canizares CA (2002) Voltage stability assessment: concepts, practices and tools. In: IEEE/PES Power System Stability Subcommittee. Final Document, Technical . Report (2002)
3. Ajjarapu V, Christy C (1992) The continuation power flow: a tool for steady state voltage stability analysis. IEEE Trans Power Syst 7(1):416–423
4. Sheng H, Chiang HD (2014) CDFLOW: a practical tool for tracing stationary behaviors of general distribution networks. IEEE Trans Power Syst 29(3):1365–1371
5. Echavarren F (2011) Formulation, computation and improvement of steady state security margins in power systems. Part I: Theoretical framework. Int J Elect Power Energy Syst 33(2):340–346
6. Gao B, Morison G, Kundur P (1992) Voltage stability evaluation using modal analysis. IEEE Trans Power Syst 7(4):1529–1542
7. Andersson G, Hill DJ (1993) Voltage stability indices for stressed power systems. IEEE Trans Power Syst 8(1):326–335
8. Yu J (2014) Identification and location of long-term voltage instability based on branch equivalent. IET Proc Gener Trans Distrib 8(1):46–54
9. Song Y, Hill DJ, Liu T (2019) Static voltage stability analysis of distribution systems based on network-load admittance ratio. IEEE Trans Power Syst 34(3):2270–2280
10. Abbas Kazmi SA, Shahzaad MK, Ryeol Shin D (2017) Voltage stability index for distribution network connected in loop configuration. IETE J Res 63(2):1–12

11. Dheer DK, Kulkarni OV, Doolla S, Rathore AK (2018) Effect of Reconfiguration and meshed networks on small signal stability margin of droop-based ıslanded microgrids, IEEE Trans Ind Appl 54(3):2821–2833
12. Shukla J, Das B, Pant V (2017) Consideration of small signal stability in multi-objective DS reconfiguration in the presence of distributed generation. IET Gen Trans Dist 11(1):236–245
13. Baran ME, Wu FF (1989) Network reconfiguration in distribution system for loss reduction and load balancing. IEEE Trans Power Del 4(2):1401–1407
14. Venkatesh B, Ranjan R, Gooi HB (2004) Optimal reconfiguration of radial distribution systems to maximize loadability. IEEE Trans Power Syst 19(1):260–266
15. Abdelaziz MMA, Farag HE, Al-Saadany EF (2016) Optimum reconfiguration of droop-controlled islanded microgrid. IEEE Trans Power Syst 31(3):2144–2153
16. Hemmatpour MH, Mohammadian M, Gharaveisi AA (2016) Optimum islanded microgrid reconfiguration based on maximization of system loadability and minimization of power losses. Electr Power Energy Syst 78:343–355
17. Mahmoud GA (2012) Voltage stability analysis of radial distribution networks using catastrophe theory. IET Gener Trans Distrib 6:612–628
18. Chakravorty M, Das D (2001) Voltage stability analysis of radial distribution networks. Int J Elec Power Energy Syst 23:129–135
19. Corsi S, Taranto GN (2008) A real-time voltage instability identification algorithm based on local phasor measurements. IEEE Trans Power Syst 23(3):1271–1279
20. Al Abri RS, El-Saadany EF, Atwa YM (2013) Optimal placement and sizing method to improve voltage stability margin in a distribution system using distributed generation. IEEE Trans Power Syst 28(1):326–334